The Fluorescence Dynamics of Single Molecules of Green Fluorescent Protein

Erwin J. G. Peterman, Sophie Brasselet, and W. E. Moerner*

Department of Chemistry, Stanford University, Stanford, California 94305-5080

Received: June 15, 1999; In Final Form: October 11, 1999

An interesting property of several yellow-emitting mutants of the green fluorescent protein (GFP) is that they switch between a fluorescent and a nonfluorescent state on a time scale of seconds. This peculiar blinking behavior was observed in single-molecule fluorescence studies of GFP mutants in poly(acrylamide) gels (Dickson, R. M.; et al. *Nature* **1997**, *388*, 355.). Utilizing primarily the yellow-emitting phenolate anion mutant EGFP, we report new single-molecule experiments studying the effect of several parameters on the blinking process: pH, host matrix, and pumping intensity. The primary measurement in these studies is the observed distribution of on-times and off-times. The on-time dynamics of EGFP are independent of pH over the range of 6−10, thus making protonation/deprotonation of the chromophore unlikely as the source of the blinking. The excitation intensity, however, has a considerable effect on the blinking: the on-times are shorter at high intensity. We compare these results to ensemble bleaching measurements which find the bleaching quantum yield of EGFP in agarose gel at pH 8 to be $(8 \pm 2) \times 10^{-6}$. The probability of termination of single-molecule emission per photon absorbed is in agreement with the bulk bleaching quantum yield, thus suggesting that the two processes are related.

Introduction

The green fluorescent protein (GFP) from the jellyfish *Aequoria victoria* and its mutants have become invaluable tools in cell biology, molecular biology, and related fields (for a recent review, see ref 1). GFP contains a strongly absorbing and highly fluorescent chromophore, which is formed by a spontaneous reaction (in the presence of oxygen) involving three amino acids (Ser65, Tyr66, and Gly67) which are part of the GFP amino acid sequence.[2] GFP is a protein, the gene of which can in principle be fused to that for any protein of choice, and no exogenous cofactor is needed to form the chromophore. Due to these characteristics, GFP has been used extensively as a reporter of gene expression,[3] a fluorescent label in order to study localization of a protein or cell organelle of choice,[1,4,5] as a pH indicator,[6,7] in a construct of two GFPs with calmodulin as Ca^{2+} indicator,[8] and even as a fluorophore for quantum control with femtosecond laser pulses.[9]

Mutations of GFP have allowed shifting of the wavelengths of optical excitation as well as generation of a wide variety of emission colors.[10,11] Of particular interest here are mutations that stabilize the phenolate anion form of the chromophore, S65T and S65G, either of which facilitates pumping with the 488 nm line of the argon ion laser. Three members of this class, S65T, S65G/S72A/T203F (denoted T203F), and S65G/S72A/T203Y (denoted T203Y), have been used successfully as chromophores for single-molecule spectroscopy, for study of GFP itself,[12] and also as probes to investigate the molecular motors kinesin[4,13,14] and myosin.[5] Single-molecule imaging has also been reported for the E222Q mutant.[15] Single-molecule fluorescence spectroscopy has proven to be an exciting and promising method for the study of several biological processes,[16,17] such as molecular motor action,[4,5] enzymatic reaction kinetics,[18] and protein structural dynamics.[19] Single-molecule experiments have potential advantages over ensemble methods in that they can provide direct information on dynamic and static disorder of (bio)molecular properties. In addition, these methods provide a way to study stochastic dynamical behavior without the need for synchronization of many molecules.[16,17] Furthermore, single-molecule methods allow statistical correlation of different molecular properties for each molecule at a time.

Often, proteins need to be labeled with fluorescent probes in order to be detectable with single-molecule fluorescence techniques. GFP and its mutants seem to be ideal candidates as probes for single-biomolecule spectroscopy, because of the ease with which a GFP fluorophore can be attached to a target protein by genetic manipulation. In cases where extremely low expression levels are of interest, the emission properties of single copies of GFP can be important. However, the GFP mutants studied so far display complex fluorescence dynamics in single-molecule experiments, which cannot be directly observed in ensemble experiments. The fluorescence from single molecules of T203Y and T203F switches on and off on a time scale of seconds (blinking) and eventually reaches a long-lived dark state, from which it can be switched back to the fluorescing state upon irradiation with 405 nm light.[12] It has been proposed that the switching is due to a transition from an anionic form of the chromophore (the emitting form) to a neutral form (not emitting).[12] For the blinking effect, a reversible transition between the emitting and another nonemitting state with unknown identity has been suggested.[12] For the S65T mutant of GFP similar effects have been observed.[13,14] This complex photophysical or photochemical behavior makes the use of GFP as single-molecule fluorescent probe challenging. To gain insight into the underlying mechanisms of the blinking effect in particular, we report in this contribution detailed studies of the single-molecule blinking behavior of several GFP mutants.

Different kinds of ensemble spectroscopic measurements on GFP and some of its mutants have revealed that the system

* Author to whom correspondence should be addressed at Department of Chemistry, Stanford University, Stanford, CA 94305-5080. Telephone: (650) 723-1727. Fax: (650) 725-0259. E-mail: w.e.moerner@stanford.edu.

10.1021/jp991968o CCC: $18.00 © 1999 American Chemical Society
Published on Web 11/09/1999

exhibits complex excited-state dynamics. First of all, GFP photobleaches like most synthetic dyes; however, to our knowledge no precise values of bleaching quantum yields have been published. No mechanism for the GFP photobleaching has been proposed, but as the bleaching rate is relatively independent of oxygen and singlet oxygen scavenger concentration, it is rather unlikely that singlet oxygen (sensitized by a GFP triplet state) is involved (as in photobleaching of many other chromophores).[1] Another interesting property of GFP is that the absorption spectrum of wild-type has two peaks, one (at 395 nm) due to the neutral form of the chromophore, the other (at 475 nm) due to the anionic form.[10,20] Detailed study of the wild-type photophysics indicates that upon illumination of the short-wavelength band, the neutral form is converted to the anionic form, which is the primary emissive state.[20,21] Quantum-chemical calculations also suggest that the different absorption peaks are due to different protonation states of the chromophore.[22−24] At the same time, some of the studies suggest that the 475 nm peak is due to the zwitterionic form of the chromophore.[24,25] Transient-absorption measurements revealed that the neutral form of the wild-type chromophore undergoes excited-state proton transfer, which is (to a large extent) reversible.[21,26]

For the GFP mutants of interest in this paper, such as EGFP (F64L/S65T), S65T, and the various S65G mutants with stacking of an aromatic residue on top of the chromophore (the so-called yellow fluorescent proteins), the anionic form of the chromophore is stabilized.[1] However, it has been shown for the S65T mutants that there is a rapid pH-dependent equilibrium ($pK_a = 5.98$) between two protonation states of the chromophore.[6,27] The state which is stable at low pH has an absorption maximum at 390 nm and is nonfluorescent. The other state is fluorescent and has an absorption maximum at 488 nm. Fluorescence correlation experiments[27] have revealed that this protonation equilibrium is fast, with time constants from 45 μs (at pH 5) to 300 μs (at pH 7). At higher pH another pH-independent process was observed (with a time constant of 340 μs), which was attributed to an internal proton-transfer process and associated conformational rearrangement.[27]

Recent quantum-chemical studies have suggested that cis/trans photoisomerization might play a role in the photochemistry (dark states) and photophysics (additional internal conversion pathways) of GFP.[22,23] These studies were motivated by the notion that the bare GFP chromophore in (liquid) solution is nonfluorescent, which has been attributed to efficient cis/trans photoisomerization, which totally quenches the fluorescence.[28] It was suggested that the chromophore, when embedded in the protein, would be locked in one conformation and thus is an efficient emitter.[28]

In this contribution we present detailed measurements of the fluorescence emission characteristics of single yellow-emitting GFP mutants which have been confined in water-filled pores of agarose and poly(acylamide) gels. We study the effect of matrix, mutation, pH, and excitation intensity and compare the single-molecule behavior to bulk experiments, to obtain insight into the photophysics and photochemistry of this system.

Materials and Methods

Sample Preparation. The GFP-mutant "EGFP" (F64L/S65T) was purchased from Clontech (Palo Alto, CA), and the mutant "10C" (S65G/V68L/Q69K/S72A/T203Y)[1] was a kind gift of Dr. Roger Tsien (Department of Pharmacology and Howard Hughes Medical Institute, University of California, San Diego). The GFP mutants were dissolved in 50 mM phosphate buffers (pH 6, 8, or 10) and embedded in water-based poly(acrylamide)[29,12] or agarose gels.[18] The poly(acrylamide) (PAA) gels were prepared by polymerizing 2 μL of a GFP/buffer solution containing 15% (weight/volume (w/v)) acrylamide and 0.5% (w/v) bis-acrylamide with ammonium persulfate (0.05% (w/v)) and *N*,*N*,*N*′,*N*′-tetramethylethylenediamine (0.3% (volume/volume)) between two cover slips. The agarose gels were prepared by adding GFP to a buffered, molten 1% (w/v) agarose (gelling point 26−30 °C, Boeringer Mannheim) and 0.1% (w/v) sodium azide solution at 40 °C. A volume of 2 μL of this molten gel was pipetted between two cover slips and allowed to cool and form a gel. For the single-molecule experiments typical GFP concentrations of 10^{-10} M were used. For the ensemble bleaching experiments a GFP concentration of 4×10^{-7} M was used.

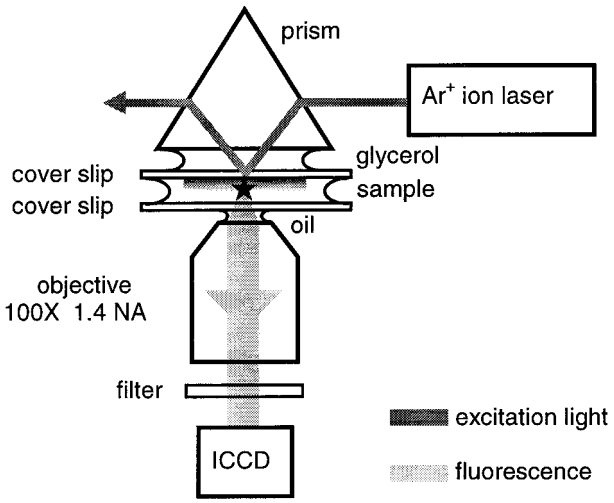

Figure 1. Schematic drawing of the TIR fluorescence microscope. See text for details.

Experimental Setups. The single-molecule fluorescence experiments forming the bulk of this work were performed using total-internal-reflection (TIR) wide-field microscopy as previously described.[12,29] A schematic drawing of the setup is shown in Figure 1. GFP-containing gels, sandwiched between two cover slips (upper one quartz, lower one glass) were mounted on a inverted microscope (Diaphot 200, Nikon). Excitation light (the 488 nm line of a Innova 200-15 (Coherent) argon-ion laser) was provided via the evanescent wave of a totally internal-reflected beam.[30] The excitation polarization contained components both parallel and perpendicular to the interface, but the specific pumping polarization is unimportant since the GFP molecules were rotating on the time scale of the experiment (vide infra). For proper angles of incidence, TIR takes place at the interface between the upper (quartz) cover slip and the sample. As is well-known,[30] the intensity of the evanescent wave drops exponentially upon penetrating the sample, with a decay length of about 150 nm for our geometry. Consequently, each molecule experiences a different excitation intensity, depending on the distance from the TIR interface. This issue will be treated in the data analysis below. The intensities quoted for the experiments (between 5 and 0.5 kW/cm^2) represent the value at the interface. Emission was collected with a 100×, 1.4 numerical aperture oil-immersion objective (PlanApo, Nikon) and imaged via a 515 nm long-pass filter and a 488 (± 20) nm band-reflect dichroic mirror (Omega Optical) on an intensified frame-transfer CCD-camera (intensified Pentamax, Princeton Instruments). With this camera 1000 emission images were recorded continuously at a frequency of 10 Hz (externally

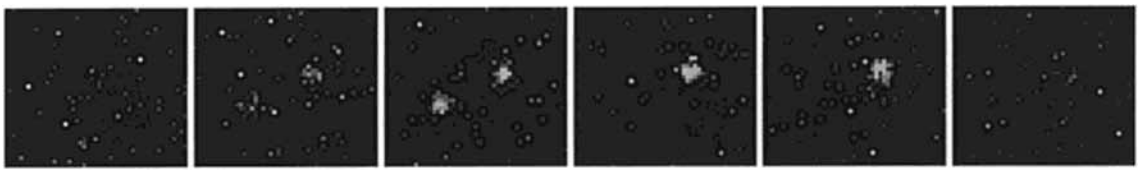

Figure 2. A typical sequence of ICCD images (2.7 by 2.3 μm) of the emission of EGFP in agarose (pH 8). The excitation intensity was 5 kW/cm^2. The integration time per frame was 100 ms.

synchronized with a function generator). From these image sequences, emission time traces were constructed by spatially integrating the ~400 nm diameter spots representing fluorescence due to single molecules.

The ensemble bleaching experiments were recorded on the same microscope with the excitation light provided via the epi-illumination port using a 488 (±20) nm band-reflect dichroic mirror (Omega Optical). The shape (Gaussian) and size (diameter 75 μm full-width at half-maximum) of the excitation spot were accurately measured at the interface, to determine excitation intensity precisely. Only the central 10 μm region of the excitation spot was imaged, to minimize the effects of variation of the excitation intensity over the spot. The emission light was filtered using a 535 (±25) nm band-pass filter (Omega Optical) and 488 nm band-reject filter (Kaiser Optical). Emission was collected in the same way as in the TIR-experiments with the intensified CCD camera. The images were integrated and time traces of the emission were constructed. The bleaching rate was calculated from the slope at zero time of the normalized time traces. The excitation rate was calculated from the excitation intensity and the absorption cross section (σ). The absorption cross section of EGFP is 2.03×10^{-16} cm^2, as calculated from the extinction coefficient at 488 nm ($\epsilon = 53\,000$ cm^{-1} M^{-1}) using $\sigma = \epsilon \cdot 2303/N_{\text{Avogadro}}$.[31]

In one experiment devised to determine the orientation of the single GFP molecules in the gel matrix, a confocal scanning microscope was utilized. Excitation light at 488 nm was provided via the epi-illumination path of the microscope (Diaphot 200, Nikon) by a 488 band-reflect dichroic mirror (Omega Optical) and then focused on the sample using a Nikon 60× 1.4 NA PlanApo oil-immersion objective. The incoming beam was made circularly polarized at the sample plane using a quarter wave plate. The excitation intensity was 0.5 kW/cm^2. The fluorescence signal was then collected by the same objective and focused on a pinhole of 50 μm diameter for confocal imaging. The optical resolution was of the order of 500 nm. The fluorescence light was filtered by a 515EFLP long-pass filter (Omega Optical), split in two perpendicularly polarized beams by a polarizing beam splitter cube (Newport), and focused on two single-photon-counting Si avalanche photodiodes (SPCM-AQ151 and -161, EG&G). The photon counts produced by both detectors were simultaneously recorded with a digital counting board (PC-TIO10, National Instruments), with an integration time of 20 ms. Molecules were selected by moving the sample with a computer-controlled piezoelectric scanner (Lumina, Topometrix). Once a molecule was detected, time traces were recorded of the fluorescence intensities in both channels. From the average intensities (during the time the molecules are emitting) in both channels the fluorescence polarization (defined as $(I_A\text{-}I_B)/(I_A+I_B)$, in which I_A and I_B are the intensities in the two channels) was calculated. A histogram was constructed from the polarization values of many single GFP molecules.

Results

A typical sequence of fluorescence images of individual EGFP molecules in (water-filled) agarose at pH 8 (excitation intensity 5 kW/cm^2) is shown in Figure 2, with time increasing from left to right, 100 ms integration time per frame. This sequence shows two molecules which are nonfluorescent in the first image and which show a burst of fluorescence during several subsequent images. This is the blinking effect which is the central focus of this paper. The typical background signal in these images is <1 (arbitrary units) per pixel, the peak signal of emission of single EGFP molecules varies from 1 to 30 per pixel, with a typical value of about 12.

From sequences of 1000 similar images, 100 s time traces of the fluorescence of single GFP molecules were extracted. We note that this parallel data acquisition method simultaneously yields data on a set of different single molecules, each at a different position in the sample. In the present study we have selected the molecules in as unbiased a fashion as possible. Some typical examples of time traces of the fluorescence of single molecules of EGFP in agarose at pH 8, with an excitation intensity of 5 kW/cm^2, are shown in Figure 3. Most molecules (86%) begin in a nonfluorescent state and show only a single burst of fluorescence lasting several frames (e.g., the top 5 traces and the bottom three traces). Some (14%) show more than one burst (e.g., trace 6 from the top) during the 100 s of observation, and a few (e.g., the bottom trace) show emission for as long as several seconds.

To analyze these time traces, we determined the duration of the fluorescence bursts, the on-times, by applying a threshold to the data. In the present study we chose to use this analysis method instead of determination of autocorrelation decay,[12] because the on-times are more straightforward to interpret and can be compared more easily with bulk experiments (see below). However, since each single copy of GFP only produces one or at most only a few events, it is not possible to measure detailed statistics of the emission from each molecule. The properties of GFP as an emitter do not allow exploration of molecule-to-molecule heterogeneity such as was possible for example for cholesterol oxidase.[18] We therefore make the reasonable assumption that the dynamical process producing the blinking is the same for all copies of EGFP in our sample, and treat all the on-time events together in the analysis. This is equivalent to the assumption made in fluorescence correlation spectroscopy when dynamics are probed by observing small numbers of molecules diffusing through a small focused laser beam.

In Figure 4 histograms of the on-times are shown for EGFP in agarose at pH 6, 8, and 10 (with excitation intensity 5 kW/cm^2). In earlier preliminary work[12] it was suggested that the single-molecule fluorescence dynamics of (other but related) GFP mutants might be due to proton rearrangements within the protein. If this is the case, then it would be expected that the pH of the solution has an influence on the blinking. Bulk fluorescence experiments showed[6,27] a pH-dependent equilibrium in EGFP between a nonemitting species absorbing at 390 nm (stable at low pH), and the emitting state absorbing at 488 nm (stable at high pH). Fluorescence correlation experiments[6,27] showed that this equilibrium takes place on a time scale of about 100 μs, depending on the pH. We cannot measure EGFP at lower pH than about 6, because of the lack of emission.

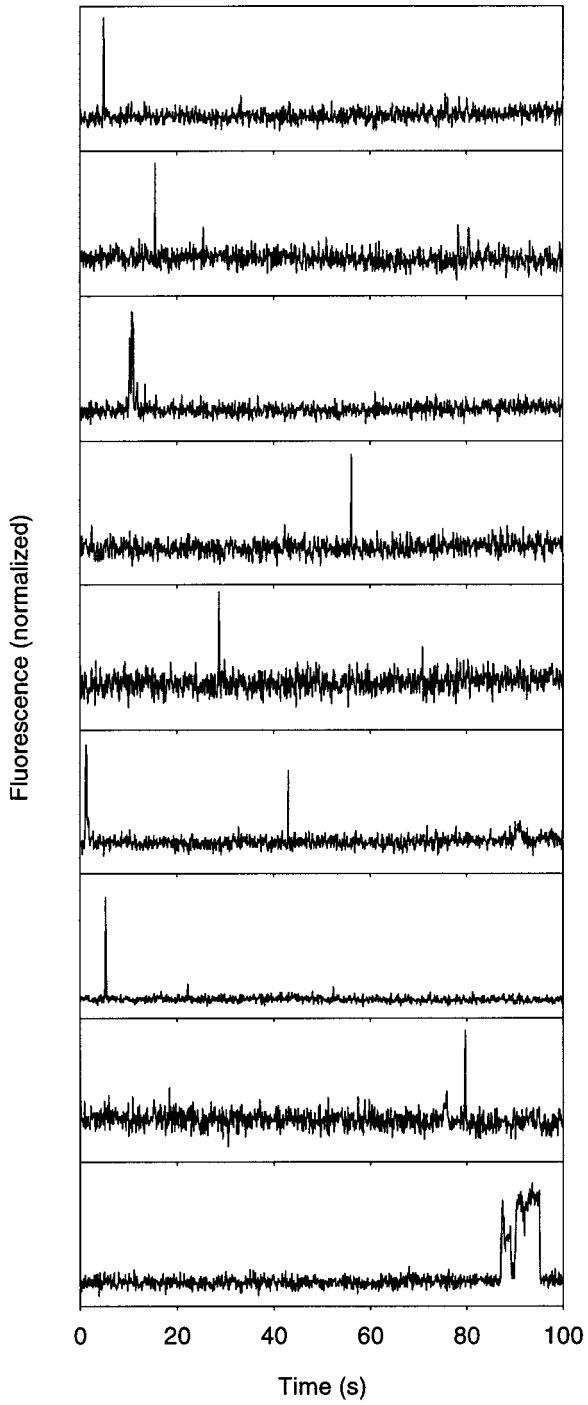

Figure 3. Typical time traces of the fluorescence of EGFP in agarose (pH 8). The excitation intensity was 5 kW/cm^2. The traces are scaled separately.

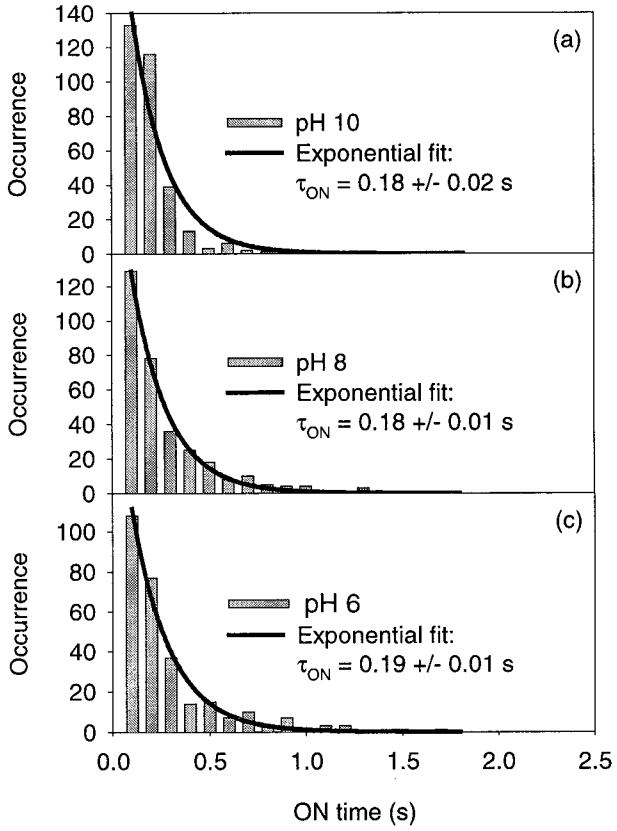

Figure 4. Histograms and exponential fits of the on-times of the fluorescence of EGFP in agarose at pH 6 (a), pH 8 (b), and pH 10 (c). In all cases the excitation intensity was 5 kW/cm^2.

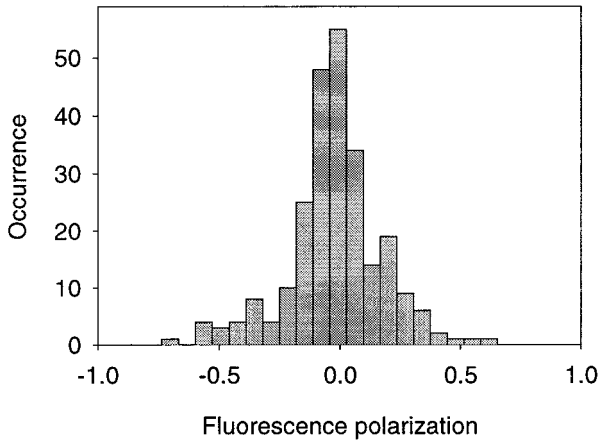

Figure 5. Histogram of the fluorescence polarization of single EGFP molecules (in agarose at pH 8) as measured with the confocal microscope (excitation intensity 0.5 kW/cm^2).

Nevertheless, since the emission is already reduced substantially at pH 6, this pH value is in fact low enough to test if the protonation equilibrium of the EGFP chromophore plays a role in the blinking. All three histograms of the EGFP on-times at different pH in Figure 4 can be fit satisfactorily with single exponential decays. The resulting characteristic decay times (τ_{ON}) are 0.18 ($\pm$0.02) s at pH 10, 0.18 ($\pm$0.01) s at pH 8, and 0.19 ($\pm$0.01) s at pH 6. The decay times are very similar for the three different pH values.

In previous single-GFP experiments of Dickson et al. the protein was immobilized in poly(acrylamide) (PAA) gel.[12] Here we chose to use agarose gels, because of the relatively larger pore size available ($\sim$200 nm[32]). Using fluorescence polarization experiments on a confocal microscope (see Figure 5) we find that the distribution of fluorescence polarizations is peaked at zero with a width that is mostly due to shot noise and background effects. This confirms that EGFP rotates in agarose gel (on a time scale much shorter than the integration time of the TIR measurements (100 ms)). Another advantage of agarose gels is that no cross-linking reaction (when GFP is already present) is needed for gel formation (unlike PAA gels[29]), which might lead to damage of GFP. In the case of agarose gels the GFP is added to a 40 °C liquid agarose solution, below the temperatures known to produce GFP unfolding, and the gel is formed upon cooling this solution to ambient room temperature.

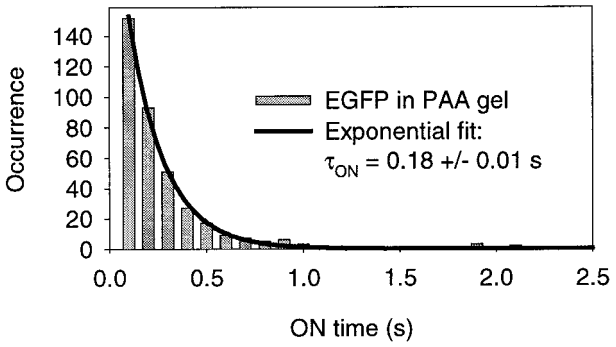

Figure 6. Histograms and exponential fits of the on-times of the fluorescence of single molecules of EGFP in PAA gel (pH 8). The excitation intensity was 5 kW/cm^2.

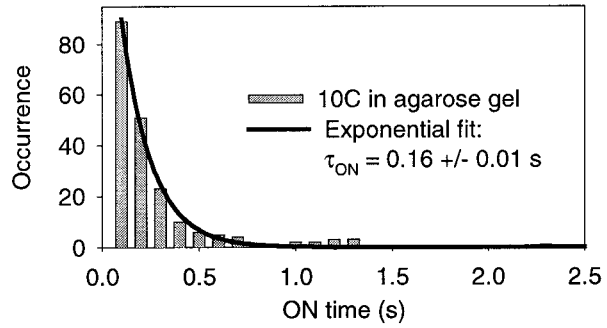

Figure 7. Histograms and exponential fits of the on-times of the fluorescence of single molecules of 10C in agarose gel (pH 8). The excitation intensity was 5 kW/cm^2.

We saw no difference in fluorescence emission and excitation spectra of EGFP in solution compared to EGFP in agarose gel (data not shown). To compare the present measurements in agarose with the previous work in PAA, we performed an experiment in the latter matrix. The result of this measurement is shown in Figure 6 and should be compared to Figure 4b (which shows the corresponding experiment in agarose gel). The histograms and the fitted (single) exponents are very similar (for both $\tau_{ON} = 0.18$ ($\pm$0.01) s), which shows that the change of matrix does not have an influence on the observed properties.

In Figure 7 the on-time histogram of the GFP mutant 10C (S65G, V68L, Q69K, S72A, T203Y) is shown. This mutant is of the yellow-fluorescent-protein class[1] which has its phenolate anion chromophore stacked with the π-electron system of tyrosine 203. The spectroscopic properties of this mutant are comparable to the yellow fluorescent proteins studied before with single-molecule spectroscopy.[12] The histogram of this mutant shows a slightly faster (single) exponential decay than the corresponding histogram of EGFP (Figure 4b) (τ_{ON}, respectively, 0.16 ($\pm$0.01) s and 0.18 ($\pm$0.01) s), showing that the difference in blinking behavior between these mutants is small, if not negligible.

We now turn to the excitation-intensity dependence of the on-time histograms. In a previous study of the single GFP mutants,[12] only weak excitation-intensity dependence was observed in the autocorrelation of the fluorescence time traces. It should be noted that studying power dependencies using TIR excitation is not straightforward: the intensity of the evanescent wave decays exponentially upon penetrating in the sample.[30] Consequently, the excitation intensity is not uniform from molecule to molecule, although large changes in excitation intensity should still affect the histograms. In Figure 8 the intensity dependence of the off-times is shown. Since few molecules exhibit multiple on-events, off-times are defined as

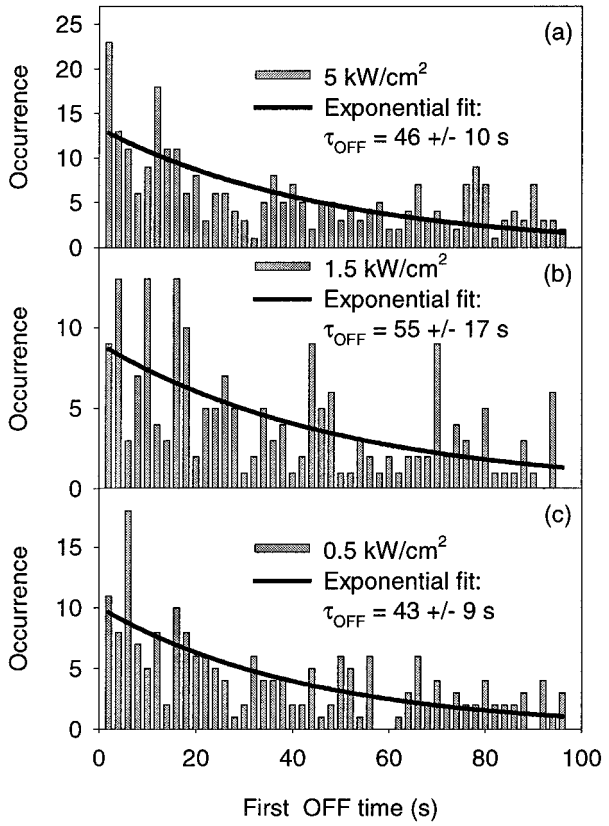

Figure 8. Histograms and exponential fits of the first off-time (i.e., the time before EGFP starts emitting) of the fluorescence of EGFP in agarose (pH 8). The excitation intensities were 5 kW/cm^2 (a), 1.5 kW/cm^2 (b), and 0.5 kW/cm^2 (c) (see text for discussion of excitation intensity in TIR).

the time between the start of the experiment and the first fluorescence burst. Therefore, the interpretation of these data must recognize that the start of the off-time interval is not the actual beginning of the off-time. The off-time histograms can be fit with single exponents. The time constants of these fits are 46 ($\pm$10) s at 5 kW/cm^2 (a), 55 ($\pm$17) s at 1.5 kW/cm^2 (b), to 43 ($\pm$9) s at 0.5 kW/cm^2 (c). These results provide no evidence that the off-times are dependent on the excitation intensity, thus it may be that the switching on of the fluorescence (i.e., the termination of the off-time) is a spontaneous process, not driven by the 488 nm pumping light. We emphasize that since the full duration of the off-time could not be observed, we are unable to draw a strong conclusion. On the other hand, the on-time histograms in Figure 9 show a weak, but clear pumping intensity dependence. The time constants of the exponential fits increase from 0.18 ($\pm$0.01) s at 5 kW/cm^2 (a), to 0.25 ($\pm$0.01) s at 1.5 kW/cm^2 (b), to 0.38 ($\pm$0.02) s at 0.5 kW/cm^2 (c).

The variation in pumping intensity from molecule to molecule may be regarded as an unfortunate type of heterogeneity in the sample induced by the TIR technique. We now show how to remove this heterogeneity by taking advantage of the fact that both the duration of each on-time and its amplitude are measured simultaneously for each molecule. The procedure involves grouping the on-time observations using the observed (emission) brightness of the molecule. Assuming that fluorescence intensity (brightness) and pumping intensity are proportional, this procedure provides us a better estimate of the pumping intensity at the location of the molecule. This assumption is met in our experiment, as the pumping intensities in our experiments are far from saturating. Furthermore, the GFP is rotating on the

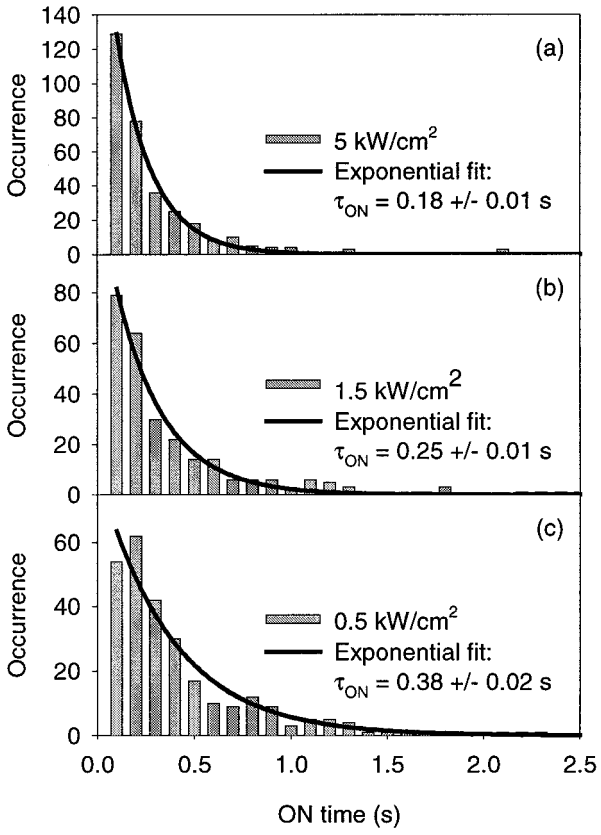

Figure 9. Histograms of the on-times of the fluorescence of EGFP in agarose (pH 8). The excitation intensities were 5 kW/cm^2 (a), 1.5 kW/cm^2 (b), and 0.5 kW/cm^2 (c) (see text for discussion of excitation intensity in TIR). Also shown are exponential fits to the histograms.

time scale of our experiments, which eliminates effects due to the polarization of the emission (fixed GFPs with a substantial *z*-component in their transition dipole moment would have appeared ring-shaped and much fainter, for example [33]). The result of this grouping by brightness of the on-times of EGFP in agarose at pH 8 is shown in Figure 10 (the histograms combine the data from all the three pumping intensities shown in Figure 9). Using this improved procedure, a much clearer pumping intensity dependence on the on-time distribution is observed: the τ_{ON} value for the brightest molecules is 0.11 ($\pm$0.01) s, that of the faintest 0.39 ($\pm$0.03) s. We conclude that the termination of the on-time is a light-driven process and that the excitation intensity dependence is stronger than suggested before.[12]

To provide insight into the behavior of EGFP at the excitation intensities used in the single-molecule experiments and to relate the single-molecule behavior to bulk experiments we studied the photobleaching of EGFP in bulk, as a function of excitation intensity. To avoid complications from diffusion, EGFP was immobilized in agarose gel (pH 8) (as in most of the single-molecule experiments). Wide-field, uniform excitation was provided via epi-illumination. The size and shape of the excitation spot were accurately determined, which allowed precise determination of the excitation intensity. In Figure 11 bleaching curves are shown at two typical excitation intensities. At 0.4 W/cm^2 (dotted line) hardly any bleaching can be observed (within the 100 s time interval shown). At 115 W/cm^2 (solid line), however, the emission bleaches quickly. From the (normalized) curves in Figure 11 the EGFP bleaching rate (i.e., the probability per second for bleaching) was determined from the initial slope of the curves. The initial slope was determined

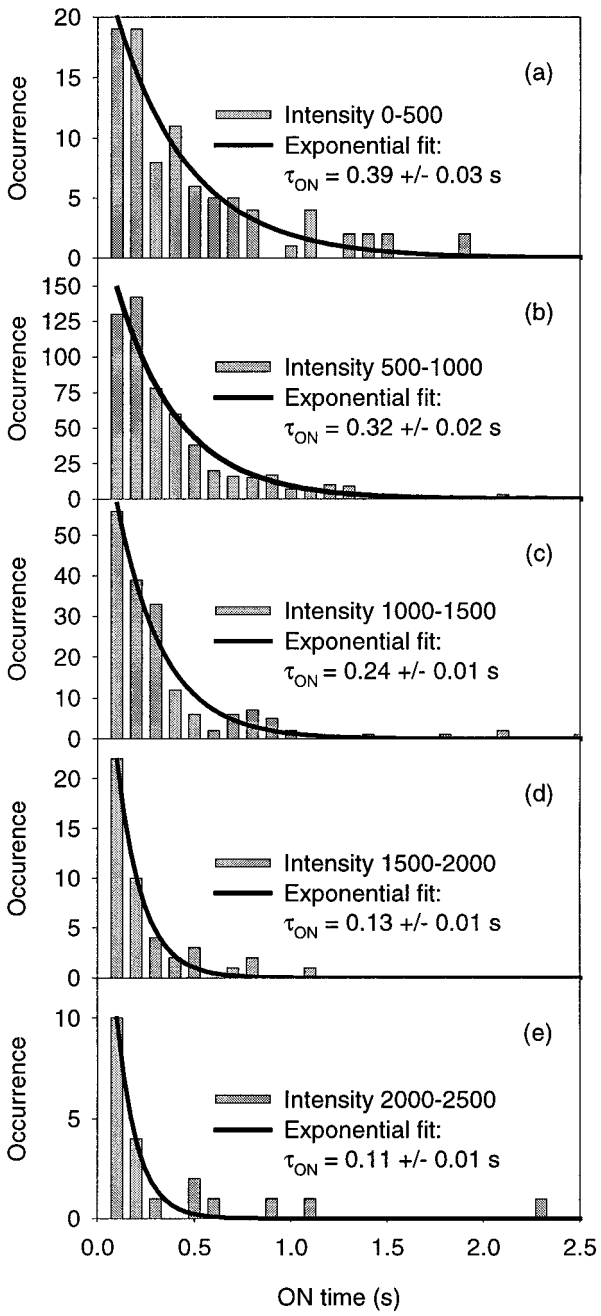

Figure 10. Emission intensity binned histograms of the on-times of the fluorescence of EGFP in agarose (pH 8) (at excitation intensities of 5 kW/cm^2, 1.5 kW/cm^2, and 0.5 kW/cm^2). The molecules were binned in five emission intensity classes (intensity in arbitrary units). Also shown are exponential fits to the histograms.

from (multi)exponential fits to the bleaching curves. In most cases two exponents and an offset were needed for a good fit, while at the lowest intensities a single exponent with offset was sufficient. In Figure 12 bleaching rates are shown as a function of excitation intensity. To determine the bleaching quantum yield, we calculated the excitation rate (i.e., the amount of absorbed photons per EGFP per second) from the excitation intensity and the absorption cross-section of EGFP (2.03×10^{-16} cm^2) (Figure 12, lower *x*-axis). The data points in Figure 12 show that the photobleaching is linearly dependent on the excitation intensity. The bleaching quantum yield of EGFP is equal to the slope of the line relating the bleaching rate to the excitation rate. A linear fit to the data in Figure 12 yields a quantum yield of photobleaching of 8 ($\pm$2) $\times$ 10^{-6}. This is

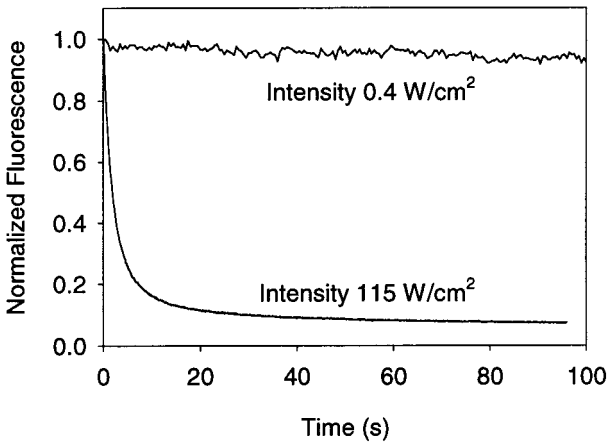

Figure 11. Ensemble bleaching curves of EGFP in agarose (pH 8) as measured with epi-illumination. The excitation intensity of the traces shown are 115 W/cm^2 and 0.4 W/cm^2. Both traces are normalized.

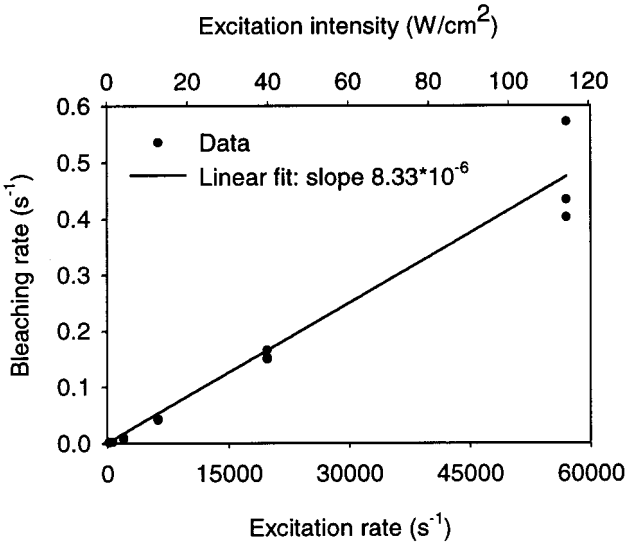

Figure 12. Ensemble bleaching rate of the fluorescence of EGFP in agarose (pH 8) as a function of the excitation rate (and excitation intensity) as measured with epi-illumination. Also shown is a linear fit to the data.

lower than that for fluorescein (2.7×10^{-5}).[34] To our knowledge, this is the first absolute determination of the photobleaching quantum yield of a GFP mutant. Previous more qualitative reports on the bleaching of GFPs compared to the dye fluorescein are contradictory. Two studies suggested that for wild-type GFP the bleaching quantum yield is considerably higher than that of fluorescein.[10,35] Another study reports photobleaching is at least 5 times slower for wild-type GFP and EGFP compared to fluorescein.[36] In our determination of the bleaching quantum yield we have carefully taken into account the excitation intensity and the extinction coefficient of EGFP, which allows a direct comparison with fluorescein.

An effective photobleaching quantum yield can also be estimated from the single-molecule data in Figure 10. The corresponding quantity is the probability of ceasing emission per photon absorbed. This probability can be estimated using $(\tau_{ON})^{-1}/R_{abs}$ where R_{abs} is the rate of photon absorption, determined from the absorption cross section of EGFP and the excitation intensity. To minimize the effect of varying pumping intensities in the evanescent field, we select τ_{ON} for the brightest molecules in Figure 11e, and assume that these have been excited with the maximum intensity (i.e., the value at the interface): 5 kW/cm^2. The resulting value for the probability of termination of emission is 3.6×10^{-6}. This value is roughly a factor of 2 smaller than the bulk bleaching quantum yield, reasonable agreement considering the uncertainty in the excitation intensity in the single-molecule experiments. This suggests that the bulk photobleaching and the short duration of the single-molecule fluorescence bursts are related and due to the same light-induced effect.

Discussion and Conclusions

We have shown that single molecules of EGFP show in most cases a single, short burst of fluorescence during 100 s of observation. For a minority of the molecules additional bursts are observed. The on-time distributions do not differ significantly in agarose from those in PAA gel. In addition, the characteristic duration of the fluorescence bursts is only slightly longer for EGFP than for another GFP mutant, 10C. The largest structural difference between these mutants is the tyrosine 203 in 10C which π-stacks with the chromophore. This π-stacked aromatic side chain causes a substantial red shift of the absorption and emission spectra of this mutant, but apparently this does not have a large effect on the temporal behavior of the single-molecule fluorescence. The duration of the single EGFP-fluorescence bursts was shown to be independent of pH (in the range of pH 6−10). The (bulk) fluorescence spectra of EGFP, however, are strongly dependent on the pH in this range: [6,27] they show a pH-dependent equilibrium between an emitting state (at pH > 6, absorbing at 488 nm) and a nonemitting state (at pH < 6, absorbing at 390 nm). Our observations suggest that it is unlikely that the blinking is due to switching between these two protonation states of the chromophore. Some other proton rearrangement, however, not accessible via change of external pH, but only caused by a low-quantum-yield excited-state proton-transfer process cannot be excluded. Other possible mechanisms might involve electron transfer or isomerization of the chromophore.[22] Finally, the on-time distributions are strongly affected by excitation intensity, which is consistent in its characteristic time with the bleaching rate extrapolated from ensemble measurements.

Since the observed dark times are very long compared to our measurement time of 100 s, less information is available on the nonemissive, dark states. It is clear, however, that the equilibrium state of the protein is the emissive form, because when a previously unirradiated region of sample is translated into view, many molecules do start out emissive. Our hypothesis of what happens in our single-molecule experiments is that during the time it takes to prepare for a computer-controlled measurement (which involves alignment and focusing), a substantial fraction of the EGFP molecules photobleaches. We have shown that the initial dark time from the beginning of the measurement until an EGFP molecule starts to emit is independent of the excitation intensity. Although not conclusive, this is consistent with the possibility that restoration of the emissive form is not light-driven (at least by 488 nm light) and therefore is spontaneous. The blinks of fluorescence we observe are due to spontaneous recovery of the emission and subsequent photobleaching. That is, the principal photobleaching effect we observe is apparently reversible for a large fraction of the EGFP molecules. It is unclear from these measurements what the photoproduct state actually is. From ensemble measurements, the bleaching rate is hardly affected by the presence of oxygen or radical scavengers.[35] This makes it unlikely that the bleaching is caused by oxidation by singlet oxygen, sensitized by triplet states, which is a common mechanism for photobleaching of chromophores. Other processes that could play a role are

electron transfer, proton rearrangement, or photoisomerization. Unfortunately, since a single molecule must emit to be observed with the current techniques, more detailed information on the nature of the dark state form is not easily obtained. Apparently spontaneous recovery from this photobleached state is possible, otherwise we would not observe the resumption of emission so easily. In addition, it has been observed that illumination with 405 nm light recovers the emission for single GFP mutants that have been placed in a long-lived dark state.[12] Such long-lived dark states and light-induced recovery processes may be the key to unraveling some of the remaining mysteries of the complex emissive behavior of green fluorescent protein mutants.

Acknowledgment. We thank R. M. Dickson for his involvement in the beginning of this project, and R. Y. Tsien for the generous gift of the 10C mutant. The research was supported by the National Science Foundation, Grant DMR-9612252 and MCB-9816947.

References and Notes

(1) Tsien, R. Y. *Annu. Rev. Biochem.* **1998**, *67*, 509−544.
(2) Prasher, D. C.; Eckenrode, V. K.; Ward, W. W.; Prendergast, F. G.; Cormier, M. J. *Gene* **1992**, *111*, 229−233.
(3) Chalfie, M.; Tu, Y.; Euskirchen, G.; Ward, W. W.; Prasher, D. C. *Science* **1994**, *263*, 802−805.
(4) Case, R. B.; Pierce, D. W.; HomBooher, N.; Hart, C. L.; Vale, R. D. *Cell* **1997**, *90*, 959−966.
(5) Iwane, A. H.; Funatsu, T.; Harada, Y.; Tokunaga, M.; Ohara, O.; Morimoto, S.; Yanagida, T. *FEBS Lett.* **1997**, *407*, 235−238.
(6) Kneen, M.; Farinas, J.; Li, Y. X.; Verkman, A. S. *Biophys. J.* **1998**, *74*, 1591−1599.
(7) Llopis, J.; McCaffery, J. M.; Miyawaki, A.; Farquhar, M. G.; Tsien, R. Y. *Proc. Natl. Acad. Sci. U.S.A.* **1998**, *95*, 6803−6808.
(8) Miyawaki, A.; Llopis, J.; Heim, R.; McCaffery, J. M.; Adams, J. A.; Ikura, M.; Tsien, R. Y. *Nature* **1997**, *388*, 882−887.
(9) Bardeen, C. J.; Yakovlev, V. V.; Squier, J. A.; Wilson, K. R. *J. Am. Chem. Soc.* **1998**, *120*, 13023−13027.
(10) Cubitt, A. B.; Heim, R.; Adams, S. R.; Boyd, A. E.; Gross, L. A.; Tsien, R. Y. *Trends Biochem. Sci.* **1995**, *20*, 448−455.
(11) Heim, R.; Cubitt, A. B.; Tsien, R. Y. *Nature* **1995**, *373*, 663−664.
(12) Dickson, R. M.; Cubitt, A. B.; Tsien, R. Y.; Moerner, W. E. *Nature* **1997**, *388*, 355−358.
(13) Pierce, D. W.; HomBooher, N.; Vale, R. D. *Nature* **1997**, *388*, 338−338.
(14) Pierce, D. W.; Vale, R. D. *Methods Cell Biol.* **1998**, *58*, 49−73.
(15) Jung, G.; Wiehler, J.; Goehde, W.; Tittel, J.; Basche, T.; Steipe, B.; Braeuchle, C. *Bioimaging* **1998**, *6*, 54−61.
(16) Moerner, W. E.; Orrit, M. *Science* **1999**, *283*, 1670−1676.
(17) Weiss, S. *Science* **1999**, *283*, 1676−1683.
(18) Lu, H. P.; Xun, L. Y.; Xie, X. S. *Science* **1998**, *282*, 1877−1882.
(19) Ha, T. J.; Ting, A. Y.; Liang, J.; Caldwell, W. B.; Deniz, A. A.; Chemla, D. S.; Schultz, P. G.; Weiss, S. *Proc. Natl. Acad. Sci. U.S.A.* **1999**, *96*, 893−898.
(20) van Thor, J. J.; Pierik, A. J.; Nugteren-Roodzant, I.; Xie, A. H.; Hellingwerf, K. J. *Biochemistry* **1998**, *37*, 16915−16921.
(21) Chattoraj, M.; King, B. A.; Bublitz, G. U.; Boxer, S. G. *Proc. Natl. Acad. Sci. U.S.A.* **1996**, *93*, 8362−8367.
(22) Weber, W.; Helms, V.; McCammon, J. A.; Langhoff, P. W. *Proc. Natl. Acad. Sci. U.S.A.* **1999**, *96*, 6177.
(23) Voityuk, A. A.; MichelBeyerle, M. E.; Rosch, N. *Chem. Phys. Lett.* **1998**, *296*, 269−276.
(24) Voityuk, A. A.; MichelBeyerle, M. E.; Rosch, N. *Chem. Phys. Lett.* **1997**, *272*, 162−167.
(25) Voityuk, A. A.; MichelBeyerle, M. E.; Rosch, N. *Chem. Phys.* **1998**, *231*, 13−25.
(26) Lossau, H.; Kummer, A.; Heinecke, R.; PollingerDammer, F.; Kompa, C.; Bieser, G.; Jonsson, T.; Silva, C. M.; Yang, M. M.; Youvan, D. C.; MichelBeyerle, M. E. *Chem. Phys.* **1996**, *213*, 1−16.
(27) Haupts, U.; Maiti, S.; Schwille, P.; Webb, W. W. *Proc. Natl. Acad. Sci. U.S.A.* **1998**, *95*, 13573−13578.
(28) Niwa, H.; Inouye, S.; Hirano, T.; Matsuno, T.; Kojima, S.; Kubota, M.; Ohashi, M.; Tsuji, F. I. *Proc. Natl. Acad. Sci. U.S.A.* **1996**, *93*, 13617−13622.
(29) Dickson, R. M.; Norris, D. J.; Tzeng, Y. L.; Moerner, W. E. *Science* **1996**, *274*, 966−969.
(30) Axelrod, D. *Methods Cell Biol.* **1989**, *30*, 245−270.
(31) Cantor, C. R.; Schimmel, P. R. *Biophysical Chemistry Part II: Techniques for the study of biological structure and function*; W. H. Freeman and company: New York, 1980.
(32) Rees, D. A. *Biochem. J.* **1972**, *126*, 257−273.
(33) Dickson, R. M.; Norris, D. J.; Moerner, W. E. *Phys. Rev. Lett.* **1998**, *81*, 5322−5325.
(34) Mathies, R. A.; Stryer, L.. In *Applications of Fluorescence in the Biomedical Sciences*; Taylor, D. L., Waggoner, A. S., Lanni, F., Murphy, R. F., Birge, R. R., Eds.; Allen R. Liss, Inc.: New York, 1986; pp 129−140.
(35) Swaminathan, R.; Hoang, C. P.; Verkman, A. S. *Biophys. J.* **1997**, *72*, 1900−1907.
(36) Patterson, G. H.; Knobel, S. M.; Sharif, W. D.; Kain, S. R.; Piston, D. W. *Biophys. J.* **1997**, *73*, 2782−2790.